Received: 5 November 2021 | Revised: 18 January 2022 | Accepted: 21 February 2022

DOI: 10.1002/jev2.12200

TECHNICAL NOTE

Lipid-based strategies used to identify extracellular vesicles in flow cytometry can be confounded by lipoproteins: Evaluations of annexin V, lactadherin, and detergent lysis

Jaco Botha[1,2,3] | **Aase Handberg**[1,2] | **Jens B. Simonsen**[3]

[1]Department of Clinical Biochemistry, Aalborg University Hospital, North Denmark Region, Aalborg, Denmark

[2]Department of Clinical Medicine, Aalborg University, Aalborg, Denmark

[3]Department of Health Technology, Technical University of Denmark, Kongens Lyngby, Denmark

Correspondence
Jaco Botha and Jens B. Simonsen, Department of Health Technology, Technical University of Denmark, Kongens Lyngby, Denmark.
Email: jabot@dtu.dk; jbak@dtu.dk

Funding information
Toyota-fonden, Denmark, Grant/Award Number: KJ/BG-8967 F

Abstract

Flow cytometry (FCM) is a popular method used in characterisation of extracellular vesicles (EVs). Circulating EVs are often identified by FCM by exploiting the lipid nature of EVs by staining with Annexin V (Anx5) or lactadherin against the membrane phospholipid phosphatidylserine (PS) and evaluating the specificity of the labels by detergent lysis of EVs. Here, we investigate whether PS labelling and detergent lysis approaches are confounded by lipoproteins, another family of lipid-based nanoparticles found in blood, in both frozen and fresh blood plasma. We demonstrated that Anx5 and lactadherin in addition to EVs stained ApoB-containing lipoproteins, identified by the use of fluorophore-labelled polyclonal ApoB-antibody, and that Anx5 had a significantly larger tendency for labelling lipoprotein-bound PS than lactadherin. Furthermore, detergent lysis resulted in a decrease in both EV and lipoprotein events and especially lipoproteins positive for either Anx5 or lactadherin. Taken together, our findings pose concerns to the use of lipid-based strategies in identifying EVs by FCM and support the use of transmembrane proteins such as tetraspannins to distinguish EVs from lipoproteins.

KEYWORDS

annexin V, chylomicrons, detergent lysis, exosomes, extracellular vesicles, flow cytometry, lactadherin, lipids, lipoproteins, phosphatidylserine, triton X-100, VLDL

1 | INTRODUCTION

Extracellular vesicles (EVs) are membrane enclosed particles released from all cells and are abundantly present in all biological fluids. In addition to a lipid bilayer membrane, EVs contain various molecular constituents including membrane and cytosolic proteins, metabolites and different species of RNAs, and their contents reflect the phenotype and state of the cells they stem from (Van Der Pol et al., 2012). Furthermore, EVs have become recognised for their potent physiological effects elicited by delivering their biomolecular cargo to recipient cells (Yáñez-Mó et al., 2015). As such, EVs have gained increased interest as biomarkers and biopharmaceuticals in the past decade. In recent years, it has become increasingly evident that the characterisation of EVs from body fluids could be complicated by contaminants in the sample. One of the major classes of contaminants is lipoproteins. Due to their physicochemical similarities to EVs specifically regarding size distributions, relative densities, and surface composition (Deguchi et al., 2000; Simonsen, 2017), and higher abundance compared to EVs in blood (Johnsen et al., 2019), isolation methods typically used for purifying EVs often result in co-purification of vast amounts of lipoproteins (De Rond et al., 2019; Sódar et al., 2016; Welton et al., 2015). This issue poses a challenge to distinguish EVs from lipoproteins with downstream characterisation methods (Johnsen et al., 2019; Mørk et al., 2017; Van Der Pol et al., 2010).

The ability of flow cytometry to characterise multiple parameters on single particles in a high-throughput manner without having to apply laborious EV isolation steps makes flow cytometry a popular method for characterising EVs in biological samples (Buzás et al., 2017; Maas et al., 2015). When using flow cytometry, EVs have traditionally been identified using labelled proteins including antibodies against EV markers or post-inserted fluorescent membrane dyes. A common marker used to denote EVs in biological fluids is the presence of phosphatidylserine (PS) on the outer leaflet of the EV-membrane. This marker has been suggested to identify a large proportion of but not all EVs (Skotland et al., 2020). Detection of PS expression on the surface of EVs has previously been achieved by labelling EV samples with fluorescently conjugated proteins known to associate with PS including Annexin V (Anx5) (Arraud et al., 2016; György et al., 2011) or lactadherin (De Rond et al., 2018; Nielsen et al., 2014).

However, although these markers are present on EVs, it is difficult to assess label specificity towards EVs, as no universal and exclusive EV marker has been identified. Currently, a common strategy used to verify EV specificity of labels in flow cytometry is the use of detergent lysis controls. Detergent lysis controls attempt to provide biological controls for EVs, as it has been demonstrated that detergents such as SDS and Triton X-100 are capable of disrupting EV-membranes (London & Brown, 2000), whereby it is hypothesised that EV-events positive for a certain marker disappear when exposed to detergents, while non-EV events remain intact (György et al., 2012; Inglis et al., 2015).

Even though the PS marker and detergent lysis approaches to identify EVs are becoming increasingly common in flow cytometry studies on EVs, few attempts have been made to validate their EV specificity. That said, lipoproteins are prone to detergent-lysis due to their lipid-nature, and lipoproteins are covered by a lipid monolayer surface that has been reported to contain PS (Bloom & Elwood, 1981; Christinat & Masoodi, 2017; Deguchi et al., 2000). Taken together, these features and the high abundance of lipoproteins in EV isolates from blood pose a question to whether these lipid-based strategies are useful tools to uniquely identify EVs.

Here, we evaluate whether the proposed PS-binding labels Anx5 and lactadherin can label lipoproteins, and whether the commonly used Triton X-100 detergent lyses lipoproteins in a flow cytometric setting. To ensure that we are able to detect lipoproteins, we used a polyclonal fluorophore-conjugated anti-ApoB-48/100 antibody to identify the largest ApoB-lipoproteins including very-low density lipoproteins (VLDL) and chylomicrons that are uniquely associated with the apolipoproteins apoB-100 (LDL and VLDL) and ApoB-48 (chylomicrons).

2 | METHODS

2.1 | Preparation of platelet-poor blood plasma

Blood was collected by a phlebotomist at the Department of Clinical Biochemistry, Aalborg University Hospital from anonymous subjects in accordance with the Helsinki Declaration and local ethical regulations upon informed consent. A pool of blood plasma was prepared from two healthy, fasting individuals. From each donor, blood was collected into BD Vacutainer™ 9NC tubes containing a final concentration of 0.0105 M NA_3 Citrate (BD Biosciences, San Jose, CA, Cat. no. 366075). Immediately after collection, platelet-poor plasma (PPP) was obtained by a two-step centrifugation protocol within one hour after collection as described previously (Lacroix et al., 2013). First, whole blood was centrifuged at 2500 × *g* for 15 min at room temperature, after which platelet-rich plasma was collected to more than 1 cm above blood cell sediment and transferred into a new tube. Second, platelet-rich plasma was subjected to an additional centrifugation cycle at 2500 × *g* for 15 min at room temperature, and PPP was collected more than 1 cm above the platelet pellet and transferred into a container, where all samples were pooled. Finally, the PPP pool was thoroughly mixed by gentle inversion and divided into 0.5 ml aliquots and stored at −80°C until use. In addition, fresh PPP was prepared as describe above from three healthy, fasting individuals and analysed the same day without being stored at −80°C.

2.2 | Preparation of lipoprotein mixtures

In order to investigate the influence of lipoproteins on flow cytometry results, commercially isolated lipoproteins (LP) were prepared diluting commercial VLDL (Lee Biosolutions; Cat.no. 365-10) or chylomicrons (Lee Biosolutions; Cat.no. 194-14) in Dulbecco's phosphate-buffered saline (PBS, Merck KGaA, Darmstadt, Germany; Cat. no. D8537-500ML; Lot. no. RNBG5293) to final concentrations of 0.625 mg/dl or 0.050 mg/dl cholesterol, respectively, based on values stated in the data sheets and after careful titration on the flow cytometer to prevent excessive background and co-particle events including swarming.

2.3 | Preparation of antibody and label master mixes

Brilliant violet 510 (BV510)-conjugated mouse monoclonal anti-CD41 (50 μg/ml; Clone HIP8; Cat. no. 563250), BV510-conjugated mouse monoclonal $IgG_1\kappa$ (200 μg/ml; Clone X40; Cat. no. 562946), cyanine 5 (Cy5)-conjugated Anx5 (16 μg/ml;

Cat. no. 559933), and Annexin binding buffer 10× (Cat. no. 556454) were purchased from BD Pharmingen, San Jose, CA, USA. Fluorescein isothiocyanate (FITC)-conjugated bovine Lactadherin (83 μg/ml; Cat. no. HALOBLAC-FITC) was purchased from Haematologic technologies Inc., VT, USA. Unconjugated goat polyclonal anti-ApoB (1 mg/ml; Cat. no. GTX27616) and unconjugated goat polyclonal IgG (1 mg/ml; Cat. no. GTX35039) were purchased from GeneTex, Irvine, CA, USA. 100 μg of goat anti-ApoB and 100 μg of goat IgG were conjugated by over-night incubation with LYNX Rapid RPE Antibody Conjugation Kits (Bio-rad, Copenhagen, DK; Cat. no LNK022RPE) and according to the manufacturer's instructions and subsequently diluted to final antibody concentrations of 100 μg/ml in PBS. Titration of all labels and antibodies were performed as described in Supplementary Figure S1.

2.4 | Labelling of samples for flow cytometry analysis

Prior to labelling, blood plasma was thawed at room temperature. Thawed PPP was subjected to a centrifugation cycle at 1850 × *g* for 5 min, after which supernatant was collected more than 0.5 cm above the bottom of the tube in order to remove clots that formed during freezing and thawing. Fresh PPP was also subjected to a centrifugation cycle at 1850 × *g* for 5 min for consistency. Lipoprotein mixtures were prepared freshly for each analysis day from frozen aliquots as described above. Prior to staining, antibody and label aggregates were removed by filtration through 0.45 μm centrifugation filters (Merck KGgA, Darmstadt, Germany, Cat. no. UFC30HV25) at 12,000 × *g* for 10 min as described by Wehner et al. (Rasmussen et al., 2021). Ten microliter of either PPP or LP were pre-diluted in 40 μl DPBS and then stained for 2 h at room temperature in the dark with 4 μl master mix consisting of anti-ApoB48/100-PE (4 μg/ml final staining concentration) and anti-CD41-BV510 (2 μg/ml final staining concentration) or isotype controls. After incubation, an additional staining step was performed with either Lactadherin-FITC or Anx5-Cy5. For Panel 1, samples were incubated for an additional 1 h at room temperature with 3.32 μg/ml Lactadherin-FITC, then diluted with DPBS to a final volume of 500 μl and moved into a dark container at room temperature. For Panel 2, 1.28 μg/ml of Anx5-Cy5 was added to samples, each diluted to a final volume of 500 μl with either Annexin binding buffer (BD Pharmingen; Cat. no. 556454) or PBS without calcium and magnesium according to the supplier's recommendations and then incubated for 1 h at room temperature in the dark.

2.5 | Flow cytometric analysis of samples

Flow cytometry was performed on an Apogee A60 Micro-PLUS flow cytometer (Apogee Flow Systems, Hemel Hempstead, UK) equipped with a 300 mW 405 nm diode laser set to 200 mW, a 180 mW 647 nm diode laser set to 100 mW, and a 200 mW 488 nm diode laser set to 100 mW. Three PMTs were factory-fitted for collection of small-angle light scatter (SALS) set to 400 V, medium-angle light scatter (MALS) set to 210 V, and large-angle light scatter (LALS) set to 400 V signals collected from the 405 nm laser after being separated from fluorescence signals on this laser by a LP415 long-pass filter. BV510 signals were collected from the 405 nm laser into a PMT set to 400 V fitted with a 525/50 bandpass filter. FITC signals were collected from the 488 nm laser into a PMT set to 400 V fitted with a 530/40 bandpass filter, PE signals were collected from the 488 nm laser into a PMT set to 400 V fitted with a 575/30 bandpass filter, and APC signals were collected from the 638 nm laser into a PMT set to 350 V fitted with a 680/35 bandpass filter. Data was acquired for 180 seconds at a constant and calibrated (volumetric syringe pump) sample flow rate of 3.01 μl/min and a sheath fluid pressure of 150 mBar in order to keep the sample core as tight as possible and allow for adequate exposure of EVs by the lasers and capture of signals in the PMTs. A triggering threshold was set on MALS to a value of 13, which corresponds to an intensity of 832 when converting the 16-bit triggering threshold to the 22-bit collection resolution, which we previously demonstrated to enable detection of 100 nm silica nanospheres on this flow cytometer (Botha et al., 2021). This setting allowed the collection of less than 100 events/s in unstained PBS. All samples were inter-spaced by flushing the sample system with double sample volumes of 20% Decon™ Contrad™ 70 liquid detergent (Decon Labs, Inc., King of Prussia, PA, USA, Cat. no. 1003) followed by an equal volume of PBS were run at a sample flow rate of 10.1 μl/min to avoid sample carry-over. Instrument settings were adjusted, and data recorded in the Histogram v. 1.21 software utility (Apogee Flow Systems). All data was acquired in the FCS v. 3.0 format and analysed in FlowJo v. 10.7.1 (FlowJo LLC, BD Biosciences, San Jose, CA).

2.6 | Controls

For each analysis day, Apogee Mix bead mixture (Apogee Flow Systems, Cat. no. 1493, Lot. no. CAL0098) for ensuring scatter signal stability, a bead mixture consisting of 100 yellow-green fluorescent silica beads excited at 405 nm and 83 nm yellow-green fluorescent polystyrene beads excited at 488 nm (Apogee Flow Systems, Cat. no. 1517, Lot. no. CAL0131) to ensure that small particles could be sufficiently detected above background (Supplementary Figure S2), and 3.4 μm fluorescent polystyrene Ultra

Rainbow Calibration particles (Spherotech, Lake Forest, IL, USA, Cat. no. RCP-30-5, Lot. no. AH01) to ensure fluorescence signal stability in all channels. In addition, unstained buffer controls and buffer controls individually stained with Panel 1 and 2 were analysed to account for background and presence of label aggregates, respectively (Supplementary Figure S3). Furthermore, single-stained controls were prepared and used to compensate for fluorescence spill-over in other channels (Supplementary Figure S4 & Table S1). In addition to daily controls, isotype control antibodies were included for all specific antibodies and prepared for both panels with Lactadherin and Anx5. For Anx5 with specific antibodies, a sample was prepared by diluting with PBS without calcium and magnesium instead of Annexin binding buffer to control for specificity of Anx5 to phosphatidylserine. Detergent lysis controls were prepared for al samples labelled with specific antibodies by incubating stained and diluted samples with Triton X-100 (Merck KGgA, Cat. no. 93443-100ML; final concentration: 1% vol/vol) for at least 30 min at room temperature in the dark. Finally, serial dilutions were prepared for both lipoprotein samples and PPP, in which samples were analysed either un-diluted or diluted 2, 4, 8, 16 or 32-fold and subsequently stained as described above. This was to investigate whether staining efficiency of ApoB+ events could be improved by further dilution as described by Sódar et al. (2016) (Supplementary Figure S5). Finally, equivalent of reference fluorophore (ERF) standardisation for PE fluorescence signals were performed using synthetic ERF-standardised fluorescent beads (Ultra Rainbow Calibration Particles; Spherotech, Lake Forest, IL, USA, Cat. no. RCP-30-5, Lot. no. AH01) according to the manufacturer's directions (Supplementary Figure S6). All controls were recorded using the same settings as for samples. More information is available in the supplementary materials and in accordance with MIFlowCyt (Lee et al., 2008) and MIFlowCyt-EV (Welsh et al., 2020) guidelines.

2.7 | NTA

Commercial lipoproteins were analysed with a nanoparticle tracking device (ZetaView PMX-420, Particle Metrix GmbH, Germany) in light scatter mode. Lipoproteins were prepared as above, and VLDL samples were further diluted 100-fold to reach a concentration that was suitable for analysis by NTA (approximately 100 particles/frame). Prior to analysis, the instrument was calibrated using yellow/green-fluorescent 100 nm polystyrene standard beads (10^6-fold dilution in 0.1 μm filtered, de-ionised H_2O). Size distributions were constructed from three exposures at 11 camera positions. Minimum brightness was set to 30 au, shutter to 100 au, minimum area to 5 au, maximum area to 1000 au, tracking radius to 100 au, and minimum track length to 15 a.u. Temperature was automatically sensed by the system, and particle size distributions were calculated based on particle Brownian motion using the Stokes–Einstein equations in the ZetaView software (version 8.05.11).

2.8 | Data analysis

Prior to compensation and gating, samples were checked for stability and consistency in flow rate and signal recordings by visually analysing the intensity of each signal over the duration of the sample analysis time and filtering out timepoints with significant shifts in median signal intensities and/or flow rates measured as particle count for timepoint. Gating (Supplementary Table S2 and Figure S3) was done separately for lipoprotein and frozen samples on the one hand, and for fresh samples on the other, as they had different levels of background fluorescence in the different fluorescent channels. Gates were constructed for each channel separately (ApoB, CD41, Anx5, lactadherin), after which double positive gates were constructed using gate 'AND' logic. Concentrations of marker-positive events was determined by dividing the number of marker-positive events with the volume of the sample analysed and adjusted for the final dilution factor.

3 | RESULTS

3.1 | Staining of lipoproteins with fluorophore-conjugated anti-ApoB-48/100

The first objective of this study was to validate whether in-house PE-conjugated commercial polyclonal anti-ApoB-48/100 antibodies could identify lipoproteins on a flow cytometer. In this study, we employed a triggering threshold on medium-angle light scatter (MALS; angle between FSC and SSC) set above background to allow collection of less than 100 events per second in unstained buffer. This triggering threshold strategy allowed us to detect down to 100 nm silica beads (refractive index (RI) = 1.4696 at 405 nm, Supplementary Figure S2), which have a similar RI to that estimated for larger lipoprotein species (Chernova et al., 2018; Van Der Pol et al., 2018). Due to the limitations of most flow cytometers to detect extremely small particles including LDL (21–27 nm), which are the most-abundant ApoB-containing particles, we used VLDL (30–80 nm) and chylomicrons (100–1000 nm) as positive controls for our in-house PE-conjugated anti-ApoB-48/100 antibody. To this end, we stained commercially available VLDL and chylomicrons with either specific anti-ApoB antibody or a matching isotype control and additionally compared these results with a buffer with antibody control.

First, we optimised the anti-ApoB antibody:ApoB protein concentration ratio in a similar fashion as described by Sódar et al. (2016) by preparing multiple serial pre-dilutions of the sample prior to staining to get an optimal binding of antibodies to and thus fluorescence signal from VLDL (Supplementary Figure S5). At the optimal anti-ApoB antibody:VLDL ratio (8-fold pre-dilution), a distinct ApoB-positive population could be distinguished from background demonstrating that the antibody was capable of detecting ApoB-particles (Figure 1a). This was additionally the case for commercial chylomicrons, in which a similar ApoB+ population could be identified, albeit with slightly higher light scatter signals on ApoB+ particles (Figure 1b). When performing serial dilutions of stained chylomicrons, the event-rate decreased proportional to the dilution (Supplementary Figure S5). Together, these features confirm that we were thus studying single VLDL and chylomicron events and not co-particle events or lipoprotein-aggregates mediated by the addition polyclonal antibodies to samples. However, if aggregation of lipoproteins follows first-order kinetics, we cannot completely exclude that lipoprotein aggregates are present in our measurements based on dilution controls.

Next, we performed the same pre-dilution experiment on frozen platelet poor plasma (PPP) as with commercial ApoB-containing lipoproteins to achieve optimal staining of ApoB (Supplementary Figure S5). We decided to use a 32-fold pre-dilution for all PPP samples (Figure 1c), as this yielded a distinct ApoB-positive population and adequate concentration of events positive for the other markers described below. Serial dilutions of PPP samples also demonstrated that the event-rate decreased proportional to the dilution factor, while the median fluorescence of ApoB+ events remained stable (Figure 1d). Like the experiments with commercial lipoproteins, this suggested that detection of ApoB-positive events was not due to coincident or swarm detection in PPP. Furthermore, events detected in the isotype (0.20% of the specifically stained VLDL sample) and buffer with ApoB-antibody controls (0.38% of the specifically stained VLDL sample) contributed very mildly to the total number of ApoB+ events in the specifically labelled sample (Supplementary Figure S3), and events in both of these controls were likely caused by antibody aggregates, which is an issue known to complicate data interpretation in small particle flow cytometry (Aass et al., 2011; Inglis et al., 2015). Thus, by using this labelling strategy, we successfully detected single ApoB-containing lipoproteins in frozen human PPP, of which only a small proportion of these events could be attributed to nonspecific binding of antibodies or antibody aggregates.

Finally, the sizes of ApoB+ events were roughly estimated in VLDL, chylomicrons and PPP using a set of silica nanospheres (RI = 1.4696 at 405 nm) whose RI closely resembles the estimated RI of larger ApoB-containing lipoproteins (RI = 1.47) (Figure 1e) (Chernova et al., 2018; Van Der Pol et al., 2018). ApoB+ events in commercial VLDL constituted a single peak whose size was between 100 nm and 180 nm silica. We expect this peak corresponds to the largest VLDL particles. Although a tail-like profile was expected as the vast majority of the VLDL size is below 80 nm, the symmetric nature of this peak is likely due to technical artefacts such as photoelectron statistics dominating the population distribution, which is pronounced at the limit of detection (Chase & Hoffman, 1998; Steen, 1992). In addition, nanoparticle tracking analysis measurements further confirmed that the commercial VLDL sample contained particles larger than 80 nm (Supplementary Figure S7). Chylomicrons, on the other hand, constituted two populations, whose sizes were between 100 nm and 180 nm silica on the one hand, and 180 nm and 590 nm silica on the other. PPP from fasting individuals yielded a population of ApoB+ events similar to that of VLDL, which constituted the majority of ApoB+ events, however a distinct population similar to what could be observed in chylomicrons could also be seen on the scatter plot of light scatter versus ApoB fluorescence (Figure 1c). Non-surprisingly, using a triggering threshold strategy on MALS (light scatter angle between forward and side scatter) arguably excludes the bulk of VLDL with sizes below 80 nm. We additionally tested a triggering strategy based on PE-fluorescence from anti-ApoB antibodies set above background (unstained buffer). However, this approach did not improve the detection of lipoproteins, and a larger proportion of triggering artefacts were included in the analysis, which could complicate the interpretation of results (Supplementary Figure S8).

3.2 | Co-staining of ApoB and different EV-markers

The second objective of this study was to investigate whether the phosphatidylserine labels Anx5 and lactadherin could stain ApoB-containing lipoproteins in blood plasma. Here, we stained a frozen PPP pool with fluorescently conjugated anti-ApoB-48/100, anti-CD41 and either Anx5 or lactadherin, where anti-CD41 labelling was used to control for non-specific staining of lipoproteins due to its specificity towards platelet-derived EVs (Phillips et al., 1988). ApoB-positive particles were found to co-stain with both Anx5 and lactadherin, while CD41 did not co-stain with ApoB-particles to a significant degree (3.4%). A large proportion of these CD41 and ApoB double-positive events could be attributed to nonspecific reactions between the two antibodies and the sample (isotype control accounts for 72.0% of events) (Figure 2a). In addition, Anx5 (43.0%) seemed to have a higher tendency to co-stain with ApoB than lactadherin (2.8%).

In order to assess whether this co-staining could be a freezing artefact arising from the destruction of residual platelets, larger EVs and lipoproteins causing membrane fragments and denatured lipoproteins to aggregate thereby giving rise to artificial double positive populations, we performed the same experiment on freshly collected blood plasma from three healthy individuals. Similar results were seen in fresh blood plasma from all three individuals as for the frozen plasma pool (Figure 2b). ApoB-positive particles were found to co-stain with Anx5 and lactadherin, while CD41 did not co-stain with ApoB to a significant degree (2.3%),

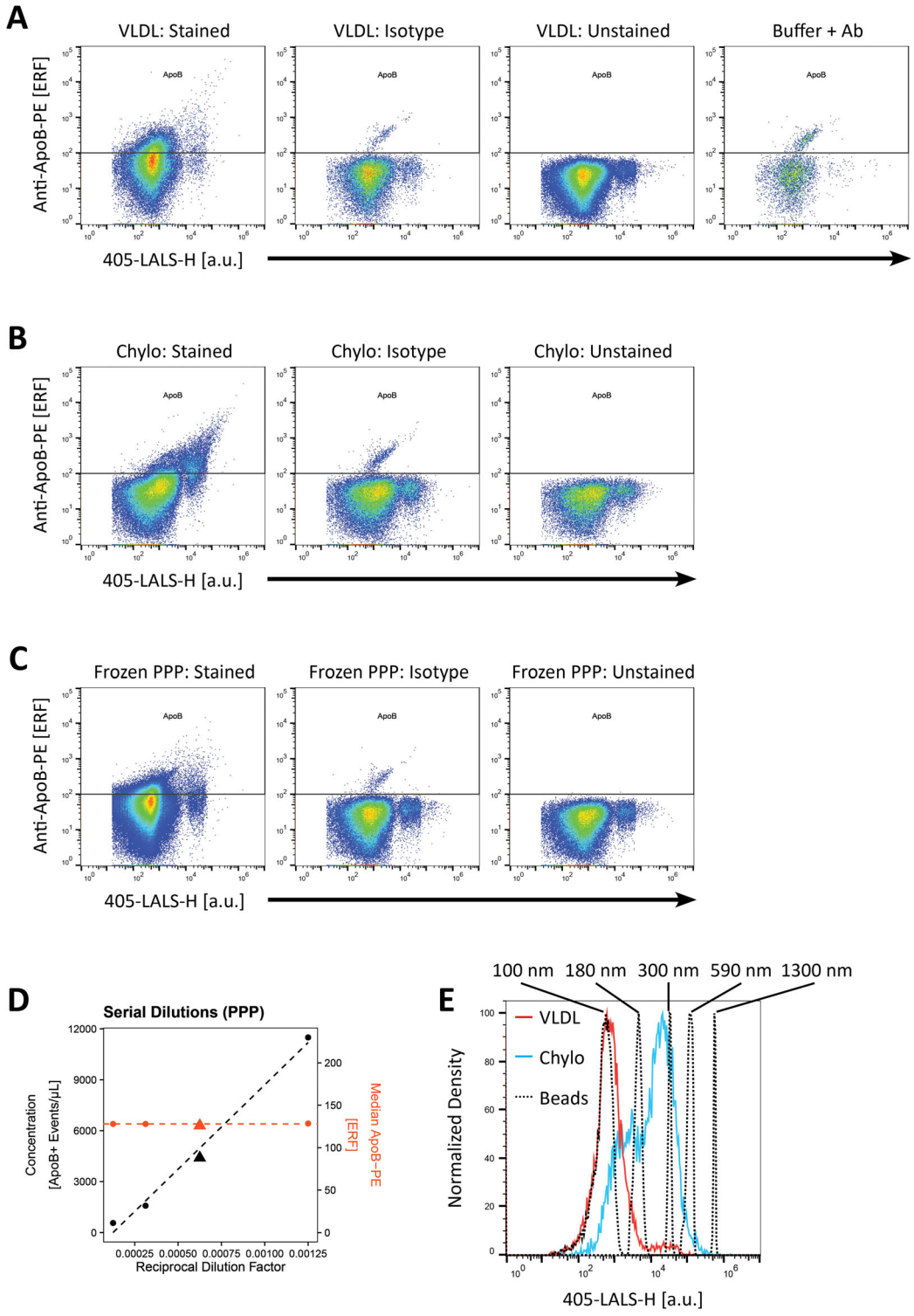

FIGURE 1 Staining of ApoB-containing lipoproteins with PE-conjugated polyclonal anti-ApoB-48/100 antibody. (a) Scatter plots depicting large-angle light scatter versus ApoB-PE fluorescence of commercial VLDL pre-diluted 8-fold and stained with fluorescent anti-ApoB antibody compared to matched isotype, unstained and buffer with reagent controls. (b) Scatter plots depicting large-angle light scatter versus ApoB-PE fluorescence of commercial chylomicrons pre-diluted 4-fold and stained with fluorescent anti-ApoB antibody compared to isotype and unstained controls. (c) Scatter plots depicting large-angle light scatter versus ApoB-PE fluorescence of platelet poor plasma (PPP) pre-diluted 32-fold and stained with fluorescent anti-ApoB antibody compared to isotype and unstained controls. Light scatter and fluorescence intensities in (A) and (B) are denoted in arbitrary units. (d) Serial dilution control of stained PPP presented with a linear relationship between ApoB event concentration not corrected for dilution factor (left y-axis, black) and reciprocal dilution factor (*x*-axis), while the median ApoB-fluorescence for ApoB-positive particles (right *y*-axis, orange) was stable. Triangles depict the dilution factor used for all subsequent experiments. (e) Light scatter distributions of ApoB-positive events in commercial VLDL (red) and chylomicrons (blue) overlayed with silica nanospheres (black, dotted) with an assumed similar RI of 1.47 to lipoproteins. Silica nanospheres from left to right: 100 nm; 180 nm; 300 nm; 590 nm; 1300 nm. ApoB: Apolipoprotein B; Chylo: Chylomicrons; LALS: Large-angle light scatter (side scatter); VLDL: Very-low density lipoprotein; Ab: Antibody; PPP: Platelet-poor plasma

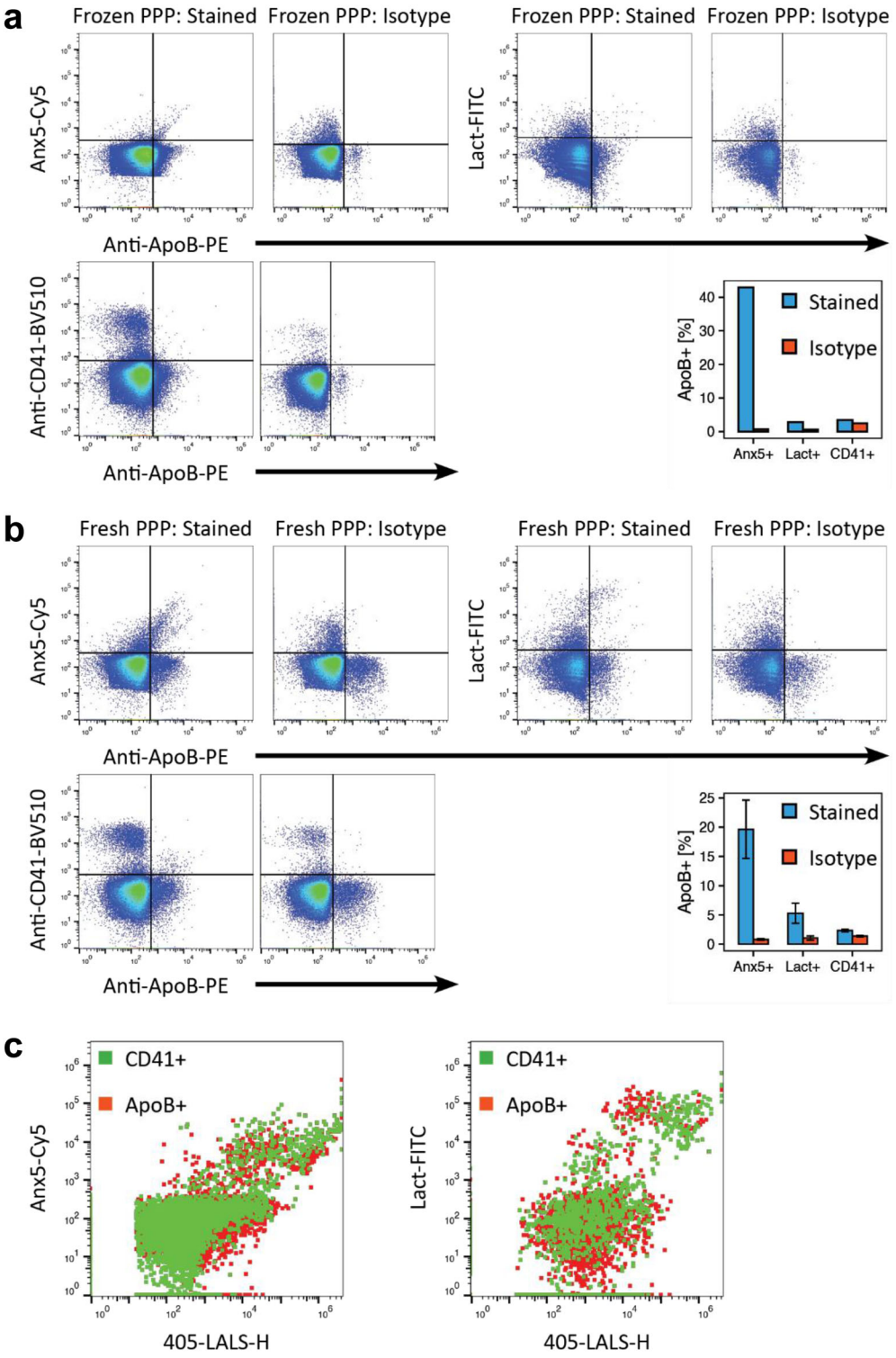

FIGURE 2 Co-staining of Anx5, lactadherin and CD41 with ApoB-containing lipoproteins. (a and b) Scatter plots of Anx5-Cy5, lactadherin-FITC and CD41-BV510 versus ApoB-PE fluorescence depicting the degree to which markers co-stain with ApoB in (a) a pool of PPP that was stored at −80°C after collection or (b) freshly collected PPP from one of three different individuals (representative data). Samples were either stained with Anx5 or lactadherin, as these markers both label PS. Bar plots depict the percentage of marker-positive events that were also positive for ApoB in specifically stained samples (blue) versus isotype controls (red). Bar plots for fresh PPP depicts the mean and standard deviation (error bars) for three individuals. (c) Dot plots (large-angle light scatter versus Anx5 or lactadherin fluorescence) of ApoB+ (red) and CD41+ (green) events demonstrate a significant overlap of these populations on these parameters. Light scatter and fluorescence intensities are denoted in arbitrary units. Anx5: Annexin V; ApoB: Apolipoprotein B; CD41: Cluster of differentiation 41/platelet membrane glycoprotein IIb-IIIa complex; Lact: Lactadherin; LALS: Large-angle light scatter (side scatter); PPP: Platelet-poor plasma

and, similar to frozen PPP, a large proportion of these events could be attributed to nonspecific reactions between ApoB and CD41 antibodies and the sample (59.3%). Likewise, Anx5 (19.6 ± 5.0%) had a higher tendency for co-staining with ApoB than Lactadherin (5.3 ± 1.7%) (Figure 2b). However, populations had markedly different profiles compared to frozen plasma, as larger particles could be observed based on light scatter and also fluorescence (Supplementary Figure S3), which is consistent with the observations that some EVs, platelets and other large entities are affected by freezing/thawing (Arraud et al., 2016; Lacroix et al., 2013; Mørk et al., 2016).

In Figure 2c, we demonstrate that events positive for both ApoB and either lactadherin or Anx5 significantly overlap with events doubly positive for CD41 and PS on SALS (forward scatter), LALS (side scatter), and lactadherin or Anx5 fluorescence channels. As such, we demonstrate that it is complicated to distinguish between EVs and lipoproteins based on any of these parameters alone or in combination with each other, and that other markers such as ApoB or EV-based membrane proteins such as CD41 are necessary to efficiently do so.

3.3 | Detergent lysis of EVs and ApoB-positive particles

The third objective of this study was to investigate whether the detergent lysis control in addition to EVs also lyses lipoproteins such as VLDL and chylomicrons. The detergent lysis control has traditionally been used to confirm the presence of true EVs in a sample, however few studies have looked at whether this control also affects lipoproteins, and, to our knowledge, no studies have looked at how lipoproteins that co-stain for lipid markers are affected by this control. Here, we incubated stained samples with Triton X-100 at a final concentration of 1% (vol/vol) for 30 minutes at room temperature and subsequently analysed these samples with the same settings as the stained samples in accordance with standard practises for lysing EVs (Tian et al., 2018).

Triton X-100 treatment of stained samples did indeed result in a subsequent decrease in the concentration of events positive for any of the markers included in this study (Figure 3a,b). Although the totality of Anx5+ events were only mildly affected by the addition of detergent to the sample (38.1% reduction), the concentration of those that co-stained with ApoB was reduced by 73.5% compared to the untreated sample. Lactadherin+ events were almost completely eliminated by the detergent (95.1% reduction), as was the population that co-stained with ApoB (88.1% reduction). The effect of the detergent was slightly less pronounced on CD41+ events than with lactadherin (72.2% reduction), however this could be a result of relatively large amounts of CD41 antibody aggregates (27.5% of positive events) being present in the sample as suggested by the buffer with antibody control. Furthermore, the detergent lysis only resulted in a mild elimination of CD41+ events that co-stained with ApoB (48.8% reduction), further suggesting that a large proportion of the CD41+|ApoB+ events are due to nonspecific interactions between antibodies and the sample, and that ApoB and CD41 are likely mutually exclusive to lipoproteins and EVs, respectively.

4 | DISCUSSION

In order to specifically identify lipoproteins, we employed a flow cytometry-based strategy in which we stained samples with fluorescently conjugated polyclonal antibody against ApoB-48/100. Although the use of polyclonal antibodies in small particle flow cytometry experiments is generally rare, we chose this strategy in order to get ample labelling of the larger ApoB-containing lipoproteins such as VLDL and chylomicrons, since each of these lipoprotein species only contains one copy of either ApoB-100 or ApoB-48 per particle, respectively (Milne & Marcel, 1982), and monoclonal antibodies would only label a single epitope on the surface of these lipoproteins, which would be insufficient for detection on flow cytometers. Further, it should be noted that ApoB-100 is a glycoprotein with a molecular mass of about 550 kDa consisting of 4536 amino acid residues, which could yield multiple epitopes for antibody binding.

First, we demonstrated that the polyclonal anti-ApoB antibody could detect commercial VLDL and chylomicrons (Figure 1a,b). These specific large lipoprotein species were chosen as controls for antibody specificity, as the light scatter triggering strategy we employed would most likely detect only chylomicrons and the largest VLDL, and smaller lipoprotein species such as LDL and smaller sized VLDL would remain undetected. We were also able to successfully detect the largest ApoB-containing lipoproteins in PPP (Figure 1c). The polyclonal anti-ApoB antibody approach used in this study has previously been described by Sódar et al. (2016), who demonstrated that these antibodies could successfully label and detect commercial LDL. Similar to the observations made by Sódar et al., we discovered that dilution of the commercial VLDL sample and both frozen and fresh PPP prior to staining was necessary in order to achieve optimal fluorescence signals from staining of lipoproteins (Supplementary Figure S5). Furthermore, we demonstrated that the identified ApoB particles were not a result of coincident event detection, as median ApoB fluorescence signal across dilution controls was stable and a linear relationship between dilution and event rate across dilutions was obtained (Figure 1d). Conversely, however, based on the light scatter-based triggering strategy used by Sódar *et al.* on a conventional flow cytometer and the resultant light scatter distribution of ApoB-containing particles, the detected ApoB-positive events in their study likely stemmed from coincident detection of LDL or multiparticle aggregates in the sample. In our study, however, we could detect single ApoB-containing lipoproteins.

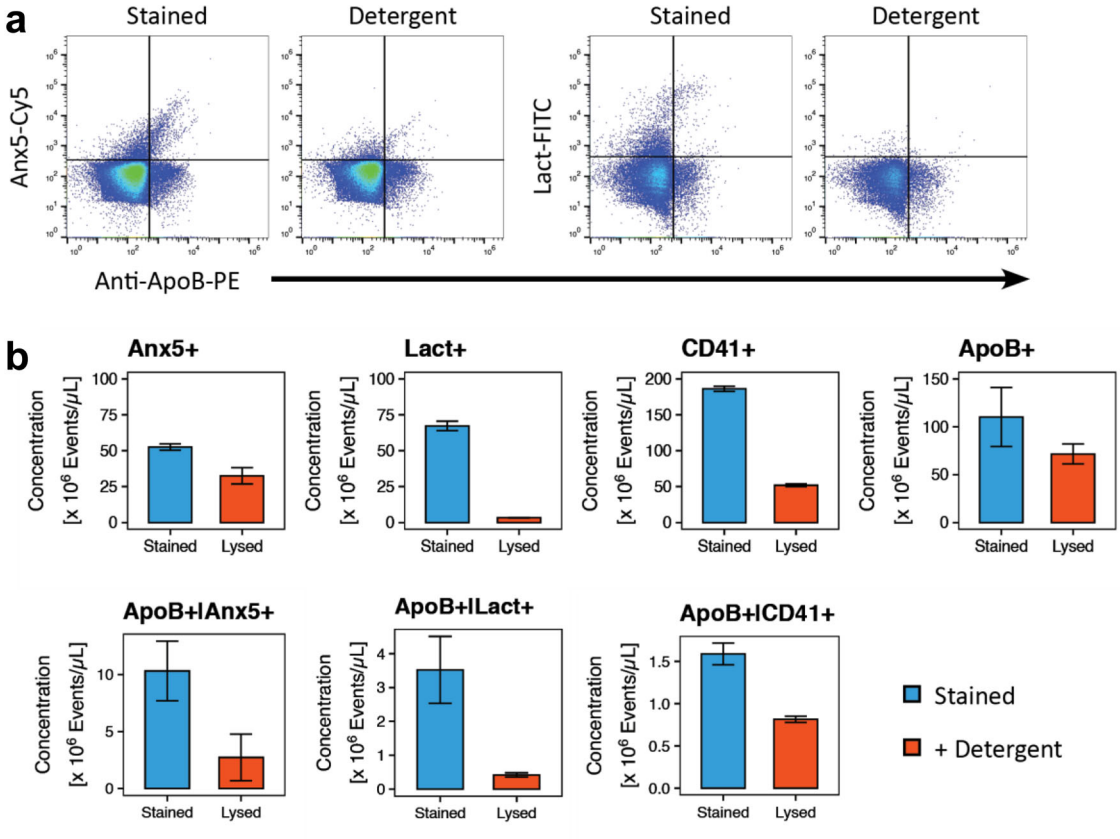

FIGURE 3 Effect of detergent lysis with Triton X-100 on ApoB-containing lipoproteins co-stained with Anx5, lactadherin and CD41. (a) Scatter plots of Anx5-Cy5 and lactadherin-FITC versus ApoB-PE fluorescence of a representative specifically stained fresh PPP sample and its detergent lysis controls depicting the degree to which the different fluorescently labelled populations are affected by detergent lysis. Fluorescence intensities is denoted in arbitrary units. (b) Bar plots of the concentrations of different marker-positive populations in specifically stained fresh PPP (blue) and detergent lysis controls (red). Bar plots for fresh PPP depict the mean and standard deviation (error bars) for three individuals. Anx5: Annexin V; ApoB: Apolipoprotein B; CD41: Cluster of differentiation 41/platelet membrane glycoprotein IIb-IIIa complex; Lact: Lactadherin

ApoB-containing lipoproteins constituted by LDL, VLDL and chylomicrons are highly abundant in blood and outnumber EVs by several orders of magnitude (Li et al., 2003). Furthermore, a several-fold higher antibody concentration compared to the number of lipoproteins is required to adequately stain each particle with multiple polyclonal antibodies to yield a high enough fluorescence signal for single ApoB-containing lipoproteins to be detected by even the most sensitive flow cytometers. Thus, based on the staining concentration of PE-labelled anti-ApoB antibody in PPP samples and assuming 10^{12} ApoB-molecules per microliter pre-diluted plasma (Johnsen et al., 2019), we estimate an antibody:ApoB ratio of 10–15 anti-ApoB per ApoB for staining our PPP samples. This was, however, somewhat lower than the lower limit of the ApoB fluorescence gate at 102 PE-molecules (determined by ERF-standardisation) and, therefore, antibodies required for particles to be defined as ApoB+ events, further assuming an ApoB antibody:fluorophore ratio of 1:1. Although there are uncertainties associated with using ERF-units as absolute numbers of fluorophores, we hypothesise that the most abundant ApoB-containing lipoproteins, LDL, are stained to a lesser degree by polyclonal ApoB antibodies compared to the larger sized VLDL and chylomicrons. First, the small size of LDL could potentially limit the binding of bulky PE-labelled antibodies with a total molecular mass of 350 kDa to a single lipoprotein. Second, the tight packing and large curvature of the large ApoB protein in LDL may also challenge binding of anti-ApoB to ApoB on LDL. To support this, it is known that many ApoA-I antibodies only recognise the denaturated ApoA-I and not native ApoA-I in the spherical small high-density lipoproteins. Furthermore, it is possible for the larger sized ApoB-containing lipoproteins including large VLDL and chylomicrons to accommodate binding of anti-ApoB differently, as the ApoB protein could likely be in a more extended conformation on chylomicrons. This could potentially explain the similarity between the PE fluorescence levels from VLDL containing one ApoB-100 and chylomicrons containing one ApoB-48, as ApoB-48 is only constituted by approximately the first 48% of amino acids in the amino-terminal of the ApoB-100 sequence. Thus, it is not impossible for single lipoproteins to be labelled with a larger number of antibodies than the proposed 10–15 anti-ApoB per ApoB molecule. We further hypothesise that the increase in number of lipoproteins with increased dilution prior to staining results from a higher antibody:antigen titre, thus yielding a higher fluorescence signal for each particle, which in turn results in more

ApoB-containing lipoproteins being detected. Regarding specificity of the anti-ApoB antibody, we consider the ApoB-staining highly specific for the ApoB-containing lipoproteins, which was confirmed by the limited number of false-positive events (i.e. ApoB+/CD41+ in Figure 2a,b). Further, serial dilutions of PPP samples confirmed that we mainly detected single particles or single aggregates that follow first-order kinetics. We further expect that the ApoB positive events are single lipoprotein events, as (i) the apparent size of the largest ApoB-containing lipoproteins is in the expected size range of chylomicrons; (ii) we do not observe an increase in Anx5 and lactadherin fluorescence intensity when the light scatter intensity increases (Figure 2c); (iii) when comparing ApoB-stained versus isotype control, there is a population that is higher on LALS in both samples. These events do, however, not increase in LALS value but they do in fluorescence; (iv) PPP stained with anti-ApoB did not differ significantly in the total number of events detected, nor did the event distribution on LALS shift compared to unstained PPP (i.e. if aggregation occurs to a significant degree, the distribution of events on LALS would be expected to differ from the unstained control; Supplementary Figure S9); and (v) we only detect a small number of CD41/ApoB positive events.

We additionally made a rough estimate of lipoprotein sizes based on light scatter signals compared to silica nanospheres (RI: 1.4696 at 405 nm), whose refractive indices are comparable to that of the larger ApoB-containing lipoproteins (1.47) (Chernova et al., 2018; Van Der Pol et al., 2018). In the commercial VLDL sample, ApoB+ events constituted a single population on large-angle light scatter (SSC) with sizes between 100 and 180 nm silica, whereas chylomicrons constituted two separate populations: one with sizes comparable to VLDL and another with sizes ranging from 180 to 590 nm silica (Figure 1e). This could potentially be explained by some VLDL being present in the commercial chylomicron sample and vice versa due to difficulties completely separating these two lipoprotein species using physicochemical methods. PPP from individuals in the fasting state contained ApoB+ events with a similar profile to commercial VLDL and, to a lesser degree, chylomicrons. In contrast to our findings, VLDL has traditionally been reported to have sizes between 30 and 80 nm (Simonsen, 2017). Our size estimation of ApoB-containing lipoproteins could be complicated for several reasons including: (i) our use of distinct RI values, as both lipoproteins and EVs have some variability in RI (Chernova et al., 2018; Van Der Pol et al., 2018), and the core in shell structure of lipoproteins is different to account for with solid silica beads (Varga et al., 2018); (ii) antibody binding to lipoproteins could affect their RI and size due to contributions by antibodies (Rupert et al., 2018); and (iii) dim signals are associated with relatively large variations in signals due to the statistical conversion of light to electrical signals (Chase & Hoffman, 1998). That said, VLDL with sizes exceeding 80 nm have been recognised, albeit with a decreasing abundance the larger the size (Li et al., 2003; Otvos et al., 1992; Wojczynski et al., 2011), which was further confirmed by our own NTA measurements of the commercial VLDL sample (Supplementary Figure S7). As mentioned above, complete separation of VLDL and chylomicrons with physicochemical methods can be complicated, and, thus, it cannot be excluded that the largest particles detected in flow cytometry and NTA in the commercial VLDL sample could be chylomicrons. Nonetheless, by using a triggering threshold on MALS (light scatter) that yields a lower particle diameter cut-off between 70 nm and 100 nm depending on particle refractive index, we therefore only detect the largest VLDL, which constitute <3% of the total VLDL population (Li et al., 2003; Wojczynski et al., 2011) and chylomicrons. Even though it has previously been suggested that triggering on fluorescence can improve the sensitivity of a flow cytometer in detecting small particles (Arraud et al., 2016), this approach yielded fewer ApoB-positive and more background events on our flow cytometer (Supplementary Figure S8).

Contrary to the use of an antibody-mediated strategy to identify lipoproteins by flow cytometry, others have used a label-free approach based on differences in light scatter profiles of particles based on their refractive index. One such method derives particle size and refractive index from the light scatter ratio between different angles (i.e. forward vs. side scatter), in which a distinction between EVs and lipoproteins is made based on their differing refractive indices (Van Der Pol et al., 2018). The light scatter ratio approach to estimate refractive index and size could have an advantage over antibody-based methods, because a large quantity of lipoproteins in a sample would either require a similarly large amount of fluorescent antibody or sample dilution prior to staining in order to yield lipoproteins that are sufficiently stained. Additionally, even with sufficient staining or dilution, some lipoproteins might still be insufficiently labelled to be discriminated from background. On the other hand, the scatter ratio approach is limited to detect particles larger than 200 nm and smaller than 500 (De Rond et al., 2019; Van Der Pol et al., 2018), a size range which is only constituted by a limited subset of chylomicrons in the case of lipoproteins. In this sense, antibody-labelling could also detect large lipoproteins larger than 100 nm and smaller than the abovementioned range. In contrast, an observed variability in the refractive index of both EVs and lipoproteins (Chernova et al., 2018; Van Der Pol et al., 2018) poses an inherent challenge to clear cut distinctions between lipoprotein and EV populations when using the light scatter ratio approach. Finally, instrument induced variabilities and sensitivity aspects are also a concern for both the biochemical and physical-based approaches for lipoprotein identification.

Next, we demonstrated that Anx5 can stain both EVs as defined by their expression of CD41, and large lipoproteins as defined by ApoB-staining. Our data (Figure 2c) shows that both the Anx5-fluorescence level and number of events were similar for ApoB-containing lipoproteins and CD41-bearing EVs. These findings challenge the use of Anx5 for uniquely identifying and enumerating EVs in samples that also contain lipoproteins. To support the notion that ApoB-containing lipoproteins contain PS, we additionally demonstrated that lactadherin, another PS-marker, also co-stained lipoproteins, albeit to a significantly lower extant than Anx5 (Figure 2a,b). This finding is in line with a recent study, which demonstrated that lactadherin also binds to lipoproteins by distinguishing between EVs and lipoproteins based on their differing refractive indices (De Rond et al., 2019).

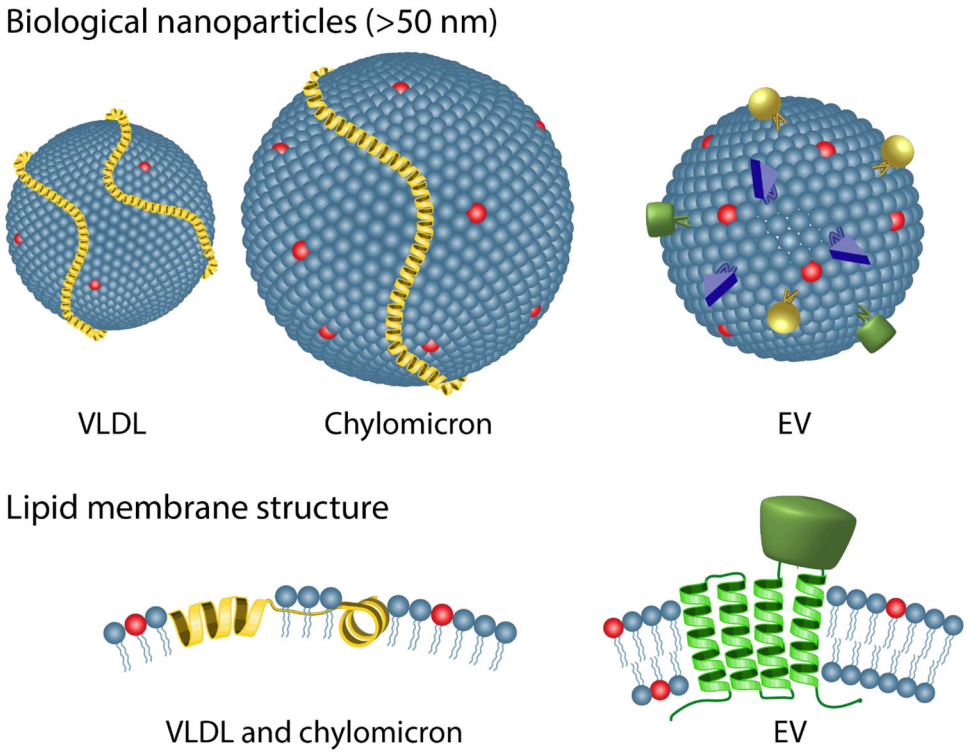

FIGURE 4 Illustrations of the similarities and differences between the large ApoB-containing lipoproteins (VLDL and chylomicrons) and EVs. The yellow alpha-helical structures on the VLDL and chylomicron represent ApoB-100 and ApoB-48, respectively. The blue spheres on all particles refer to phospholipids while the red spheres represent PS phospholipids. The additional coloured components on the EV represent different types of membrane proteins such as tetraspannins (green). Cholesterol and other membrane components including other types of apolipoproteins on the lipoproteins have been left out for the sake of simplicity

Nonetheless, it is notable that a larger proportion of Anx5+ events were also positive for ApoB than lactadherin+ events. This could, in part, be explained by lactadherin having a preference for large curvatures (smaller spherical particles) (Otzen et al., 2012; Shi et al., 2004). Furthermore, its specificity for PS has been shown to be nearly abolished on monolayer membrane surfaces such as micelles (Otzen et al., 2012), thereby making it more unlikely to label lipoproteins, which are covered by a monolayer of phospholipids (Figure 4). In contrast, Anx5 has been shown to have a higher affinity for PS on membranes with a lower curvature (larger particles) (Andree et al., 1992) and affinity to PS on phospholipid monolayer surfaces in the presence of Ca^{2+} (Meers & Mealy, 1994; Pigault et al., 1994). Another interesting observation was that Anx5 and especially lactadherin fluorescence intensities were generally high on ApoB+ events. Although we do not fully understand this phenomenon, we speculate that this could be due to differences in their binding mechanisms including curvature effects, binding cooperativity, less complex surface composition, and differences in the fluorophore intensities between Cy5 and FITC.

While the presence of PS in EV membranes is widely agreed upon (Arraud et al., 2014, 2015, 2016; De Rond et al., 2018), its presence in different lipoprotein species is somewhat more contested. Although some studies have failed to detect PS in lipoprotein fractions (Dashti et al., 2011), several studies support our findings that that PS is present in lipoproteins including LDL (Bloom & Elwood, 1981; Christinat & Masoodi, 2017; Deguchi et al., 2000), VLDL (Bloom & Elwood, 1981; Deguchi et al., 2000) and chylomicrons (Crawford & Borensztajn, 1999; Yang et al., 1992). That said, the assessment of the PS content in lipoproteins is in general confronted with several challenges as different methods used for lipoprotein isolation, lipid extraction and lipid determination are associated with different levels of contamination and yields, bias for certain lipids and exhibit different sensitivity and specificity, respectively. It is notable that lipidomic studies using mass spectrometry operating in the positive ionisation mode cannot detect the negatively charged PS lipids (Kaabia et al., 2018). On top of that, the variability across human individuals also introduces different results acquired across studies. To add to the complexity of the PS content associated with lipoproteins, the lipid-based particles like EVs and lipoproteins are dynamic entities. We recently showed that fluorophore anchored lipids incorporated into synthetic high-density lipoproteins (HDL) and synthetic vesicles (liposomes) can exchange with endogenous components in serum and plasma (Münter et al., 2018; Pedersbæk et al., 2019). Interestingly, we were able to show that the lipid exchange between synthetic HDL and endogenous lipoproteins can be mediated by direct interactions between the particles in a non-enzymatic fashion (Pedersbæk et al., 2019). Thus, although ApoB-containing lipoproteins could be synthesised in vivo without PS, collisions between lipoproteins on the one hand, and EVs and cells on the other could potentially remodel the

surface lipid composition of lipoproteins by which the presence of PS could be conferred to the surface of these ApoB-containing lipoproteins.

The detergent lysis control has become a popular addition in flow cytometry experiments due to its perceived ability to distinguish between EVs and other confounding particles present in the sample that could exhibit similar properties to EVs (Osteikoetxea et al., 2015). In this study, however, we demonstrated that Triton X-100 successfully lyses EVs and a significant number of ApoB-containing lipoproteins (Figure 3). Previously, Sódar et al. (2016) demonstrated that lipoproteins were also sensitive to detergent lysis, as their concentrations decreased following treatment with Triton X-100. We further demonstrated that ApoB-containing lipoproteins positive for the binding of lactadherin and Anx5 were affected to a higher degree than the ApoB-positive population as a whole and similar to that of EVs. We additionally demonstrated that Anx5-positive and lactadherin-positive events had different detergent sensitivities, which could suggest that these markers stain different populations of EVs (Osteikoetxea et al., 2015). Nonetheless, these results raise a concern that the detergent lysis control does not provide ample evidence for the EV origin of markers such as PS and other phospholipids that could also be present on lipoproteins.

Lipoproteins are a class of varying species of sub-micron assemblies of protein and lipids abundantly present in blood that have commonly been demonstrated to co-isolate with and interfere with characterisation of EVs due to several physical and biochemical similarities (discussed in Simonsen, 2017). Lipoproteins are also lipid-based particles with both similar and dissimilar physicochemical characteristics to EVs (Figure 4), and this study further highlights that these particles also interact with the lipid-based EV identifiers. Since lipoproteins are much more abundant than EVs in blood (Johnsen et al., 2019) and exhibit sizes and densities that are overlapping with EVs (Simonsen, 2017), a careful evaluation in terms of EV and lipoprotein sensitivity and specificity should be performed when lipid-based approaches for EV identification are used. For example, when estimating the EV concentration based on Anx5 positive events, an assessment on whether the lipoproteins go under or over the detection limit should be conducted to assess whether and to what extent lipoproteins add to the derived EV concentration. Taking the similarity of EVs and lipoproteins in terms of lipid composition into account, our work supports the use of membrane-spanning proteins such as CD9, CD63 and CD81 or phenotype specific proteins for EV identification by flow cytometry either on their own or in combination with generic markers such as Anx5 or lactadherin, as these membrane-bound proteins cannot exist in the lipoprotein lipid-monolayer surface (Figure 4). Alternatively, a similar ApoB labelling strategy to the one presented in this study could be used to identify ApoB-containing lipoproteins to either account for the extent of confounding or to remove them from the data set completely (gate-out strategy), albeit with some caveats as discussed above.

In summary, flow cytometry is a popular method used for characterisation of EVs. Lipid-targeting strategies such as labelling of specific membrane lipids and lysis of membranes are commonly used to define EVs or control for contaminants in the sample. Here, we highlight that lipoproteins can interfere with flow cytometric characterisation of EVs when lipid-based strategies are used to define EVs. We present new evidence that suggests that both Anx5 and lactadherin, two highly used markers for detection of PS-expression on the surface of EVs, also label ApoB-containing lipoproteins. This result further strengthens the findings from MS-based studies that lipoproteins contain some level of PS. We also show that the commonly used detergent lysis control for identifying EV-specific events in flow cytometry also affects some lipoprotein populations to a similar extent, which could complicate result interpretation. Both of these lipid-based approaches (selective labelling of PS-markers and detergent lysis of lipid membranes) for EV identification exploit the lipid-nature of EVs, but as illustrated herein, these approaches can be confounded by the lipid-nature of lipoproteins. Towards distinguishing EVs from lipoproteins, we discuss the merits and challenges of using physical (light scatter-based) and biochemical (antibody-based) strategies for identifying and differentiating EVs from lipoproteins in flow cytometry.

ACKNOWLEDGEMENTS

The authors would like to acknowledge Dr. Joshua A. Welsh for the valuable inputs he provided. Furthermore, the authors would like to acknowledge Rikke W. Rasmussen for coordinating collection of samples for this study. Finally, the authors would like to thank Katrine Jønsson for assisting with NTA measurements of commercial lipoproteins. This work has been supported by the Toyota-fonden, Denmark (KJ/BG-8967 F).

CONFLICTS OF INTEREST

The authors declare no conflicts of interest.

AUTHOR CONTRIBUTIONS

Conceptualization, J.B., J.B.S.; methodology, J.B., J.B.S.; validation, J.B., J.B.S.; formal analysis, J.B., J.B.S.; investigation, J.B., J.B.S.; resources, J.B., A.H., J.B.S.; data curation, J.B.; writing—original draft preparation, J.B., J.B.S; writing—review and editing, J.B., A.H., J.B.S.; visualization, J.B.; supervision, A.H., J.B.S.; project administration, J.B., J.B.S.; funding acquisition, A.H. All authors have read and agreed to the published version of the manuscript.

DATA AVAILABILITY STATEMENT

All data produced in this study can be obtained on reasonable request from Jaco Botha (jabot@dtu.dk).

ORCID

Jaco Botha https://orcid.org/0000-0002-8889-9959
Jens B. Simonsen https://orcid.org/0000-0002-4797-8570

REFERENCES

Aass, H. C. D., Øvstebø, R., Trøseid, A-M. S., Kierulf, P., Berg, J. P., & Henriksson, C. E. (2011). Fluorescent particles in the antibody solution result in false TF- and CD14-positive microparticles in flow cytometric analysis. *Cytometry Part A: The Journal of the International Society for Analytical Cytology*, *79*(12), 990–999. https://doi.org/10.1002/cyto.a.21147

Andree, H. A., Stuart, M. C., Hermens, W. T., Reutelingsperger, C. P., Hemker, H. C., Frederik, P. M., & Willems, G. M. (1992). Clustering of lipid-bound annexin V may explain its anticoagulant effect. *The Journal of Biological Chemistry*, *267*(25), 17907–17912. https://doi.org/10.1016/s0021-9258(19)37128-5

Arraud, N., Gounou, C., Linares, R., & Brisson, A. R. (2015). A simple flow cytometry method improves the detection of phosphatidylserine-exposing extracellular vesicles. *Journal of Thrombosis andHaemostasis: JTH*, *13*(2), 237–247. https://doi.org/10.1111/jth.12767

Arraud, N., Gounou, C., Turpin, D., & Brisson, A. R. (2016). Fluorescence triggering: A general strategy for enumerating and phenotyping extracellular vesicles by flow cytometry. *Cytometry Part A : The Journal of The International Society for Analytical Cytology*, *89*(2), 184–195. https://doi.org/10.1002/cyto.a.22669

Arraud, N., Linares, R., Tan, S., Gounou, C., Pasquet, J. - M., Mornet, S., & Brisson, A. R. (2014). Extracellular vesicles from blood plasma: Determination of their morphology, size, phenotype and concentration. *Journal of thrombosis and haemostasis : JTH*, *12*(5), 614–627. https://doi.org/10.1111/jth.12554

Bloom, R. J., & Elwood, J. C. (1981). Quantitation of lipid profiles from isolated serum lipoproteins using small volumes of human serum. *Clinical Biochemistry*, *14*(3), 119–125. https://doi.org/10.1016/s0009-9120(81)90239-3

Botha, J., Pugsley, H. R., & Handberg, A. (2021). Conventional, high-resolution and imaging flow cytometry: Benchmarking performance in characterisation of extracellular vesicles. *Biomedicines*, *9*(2), 124. https://doi.org/10.3390/biomedicines9020124

Buzás, E. I., Gardiner, C., Lee, C., & Smith, Z. J. (2017). Single particle analysis: Methods for detection of platelet extracellular vesicles in suspension (excluding flow cytometry). *Platelets*, *28*(3), 249–255. https://doi.org/10.1080/09537104.2016.1260704

Chase, E. S., & Hoffman, R. A. (1998). Resolution of dimly fluorescent particles: A practical measure of fluorescence sensitivity. *Cytometry*, *33*(2), 267–279. https://doi.org/10.1002/(SICI)1097-0320(19981001)33:2<267::AID-CYTO24>3.0.CO;2-R

Chernova, D. N., Konokhova, A. I., Novikova, O. A., Yurkin, M. A., Strokotov, D. I., Karpenko, A. A., Chernyshev, A. V., & Maltsev, V. P.(2018). Chylomicrons against light scattering: The battle for characterization. *Journal of Biophotonics*, *11*(10), e201700381. https://doi.org/10.1002/jbio.201700381

Christinat, N., Masoodi, M. (2017) Comprehensive lipoprotein characterization using lipidomics analysis of human plasma. *Journal of Proteome Research*, *16*(8), 2947–2953. https://doi.org/10.1021/acs.jproteome.7b00236

Crawford, S. E., & Borensztajn, J. (1999). Plasma clearance and liver uptake of chylomicron remnants generated by hepatic lipase lipolysis: Evidence for a lactoferrin-sensitive and apolipoprotein E-independent pathway. *Journal of Lipid Research*, *40*(5), 797–805. https://doi.org/10.1016/s0022-2275(20)32114-3

Dashti, M., Kulik, W., Hoek, F., Veerman, E. C., Peppelenbosch, M. P., & Rezaee, F. (2011). A phospholipidomic analysis of all defined human plasma lipoproteins. *Scientific Reports*, *1*, 139. https://doi.org/10.1038/srep00139

De Rond, L., Libregts, S. F. W. M., Rikkert, L. G., Hau, C. M., Van Der Pol, E., Nieuwland, R., Van Leeuwen, T. G., & Coumans, F. A. W. (2019). Refractive index to evaluate staining specificity of extracellular vesicles by flow cytometry. *Journal of Extracellular Vesicles*, *8*(1), 1643671. https://doi.org/10.1080/20013078.2019.1643671

De Rond, L., Van Der Pol, E., Hau, C. M., Varga, Z., Sturk, A., Van Leeuwen, T. G., Nieuwland, R., & Coumans, F. A. W. (2018). Comparison of generic fluorescent markers for detection of extracellular vesicles by flow cytometry. *Clinical Chemistry*, *64*(4), 680–689. https://doi.org/10.1373/clinchem.2017.278978

Deguchi, H., Fernandez, J. A., Hackeng, T. M., Banka, C. L., & Griffin, J. H. (2000). Cardiolipin is a normal component of human plasma lipoproteins. *Proceedings of the National Academy of Sciences of the United States of America*, *97*(4), 1743–1748. https://doi.org/10.1073/pnas.97.4.1743

György, B., Módos, K., & Pállinger, E. (2011). Detection and isolation of cell-derived microparticles are compromised by protein complexes resulting from shared biophysical parameters. *Blood*, *117*(4), e39–48. https://doi.org/10.1182/blood-2010-09-307595

György, B., Szabó, T. G., Turiák, L., Wright, M., Herczeg, P., Lédeczi, Z., Kittel, Á., Polgár, A., Tóth, K., Dérfalvi, B., Zelenák, G., Böröcz, I., Carr, B., Nagy, G., Vékey, K., Gay, S., Falus, A., & Buzás, E. I. (2012). Improved flow cytometric assessment reveals distinct microvesicle (cell-derived microparticle) signatures in joint diseases. *PloS One*, *7*(11), e49726. https://doi.org/10.1371/journal.pone.0049726

Inglis, H. C., Danesh, A., Shah, A., Lacroix, J., Spinella, P. C., & Norris, P. J. (2015). Techniques to improve detection and analysis of extracellular vesicles using flow cytometry. *Cytometry Part A : The Journal of The International Society for Analytical Cytology*, *87*(11), 1052–1063. https://doi.org/10.1002/cyto.a.22649

Johnsen, K. B., Gudbergsson, J. M., Andresen, T. L., & Simonsen, J. B. (2019). What is the blood concentration of extracellular vesicles? Implications for the use of extracellular vesicles as blood-borne biomarkers of cancer. *Biochimica et Biophysica Acta Reviews on Cancer*, *1871*(1), 109–116. https://doi.org/10.1016/j.bbcan.2018.11.006

Kaabia, Z., Poirier, J., Moughaizel, M., Aguesse, A., Billon-Crossouard, S., Fall, F., Durand, M., Dagher, E., Krempf, M., & Croyal, M. (2018). Plasma lipidomic analysis reveals strong similarities between lipid fingerprints in human, hamster and mouse compared to other animal species. *Scientific Reports*, *8*(1), 15893. https://doi.org/10.1038/s41598-018-34329-3

Lacroix, R., Judicone, C., Mooberry, M., Boucekine, M., Key, N. S., & Dignat-George, F. (2013). Standardization of pre-analytical variables in plasma microparticle determination: Results of the International Society on Thrombosis and Haemostasis SSC Collaborative workshop. *Journal of Thrombosis and Haemostasis: JTH 11*(6), 1190–1193. https://doi.org/10.1111/jth.12207

Lee, J. A., Spidlen, J., Boyce, K., Cai, J., Crosbie, N., Dalphin, M., Furlong, J., Gasparetto, M., Goldberg, M., Goralczyk, E. M., Hyun, B., Jansen, K., Kollmann, T., Kong, M., Leif, R., Mcweeney, S., Moloshok, T. D., Moore, W., Nolan, G., & …, Brinkman, R. R. (2008). MIFlowCyt: The minimum information about a Flow Cytometry Experiment. *Cytometry Part A: The Journal of the International Society for Analytical Cytology*, *73*(10), 926–930. https://doi.org/10.1002/cyto.a.20623

Li, Z., Otvos, J. D., Lamon-Fava, S., Carrasco, W. V., Lichtenstein, A. H., Mcnamara, J. R., Ordovas, J. M., & Schaefer, E. J. (2003).et al Men and women differ in lipoprotein response to dietary saturated fat and cholesterol restriction. *The Journal of Nutrition*, *133*(11), 3428–3433. https://doi.org/10.1093/jn/133.11.3428

London, E., Brown, D A. (2000) Insolubility of lipids in triton X-100: physical origin and relationship to sphingolipid/cholesterol membrane domains (rafts). *Biochimica et Biophysica Acta*, *1508*(1–2), 182–195. https://doi.org/10.1016/s0304-4157(00)00007-1

Maas, S. L.N., De Vrij, J., Van Der Vlist, E. J., Geragousian, B., Van Bloois, L., Mastrobattista, E., Schiffelers, R. M., Wauben, M. H.M., Broekman, M. L.D., & Nolte-'T Hoen, E. N.M. (2015).et al Possibilities and limitations of current technologies for quantification of biological extracellular vesicles and synthetic mimics. *Journal of Controlled Release: Official Journal of the Controlled Release Society*, *200*, 87–96. https://doi.org/10.1016/j.jconrel.2014.12.041

Meers, P., Mealy, T. (1994) Phospholipid determinants for annexin V binding sites and the role of tryptophan 187. *Biochemistry*, *33*(19), 5829–5837. https://doi.org/10.1021/bi00185a022

Milne, R. W., & Marcel, Y. L. (1982). Monoclonal antibodies against human low density lipoprotein. Stoichiometric binding studies using Fab fragments. *FEBS Letters*, *146*(1), 97–100. https://doi.org/10.1016/0014-5793(82)80712-6

Mørk, M., Handberg, A., Pedersen, S., Jørgensen, M. M., Bæk, R., Nielsen, M. K., & Kristensen, S. R. (2017).et al Prospects and limitations of antibody-mediated clearing of lipoproteins from blood plasma prior to nanoparticle tracking analysis of extracellular vesicles. *Journal of Extracellular Vesicles*, *6*(1), 1308779. https://doi.org/10.1080/20013078.2017.1308779

Mørk, M., Pedersen, S., Botha, J., Lund, S. M., & Kristensen, S. R. (2016). Preanalytical, analytical, and biological variation of blood plasma submicron particle levels measured with nanoparticle tracking analysis and tunable resistive pulse sensing. *Scandinavian Journal of Clinical and Laboratory Investigation*, *76*(5), 349–360. https://doi.org/10.1080/00365513.2016.1178801

Münter, R., Kristensen, K., Pedersbæk, D., Larsen, J. B., Simonsen, J. B., & Andresen, T. L. (2018). Dissociation of fluorescently labeled lipids from liposomes in biological environments challenges the interpretation of uptake studies. *Nanoscale*, *10*(48), 22720–22724. https://doi.org/10.1039/c8nr07755j

Nielsen, M. H., Beck-Nielsen, H., Andersen, M. N., & Handberg, A. (2014). A flow cytometric method for characterization of circulating cell-derived microparticles in plasma. *Journal of Extracellular Vesicles*, *3*, 1–12. https://doi.org/10.3402/jev.v3.20795

Osteikoetxea, X., Sódar, B., & Németh, A. (2015). Differential detergent sensitivity of extracellular vesicle subpopulations. *Organic & Biomolecular Chemistry*, *13*(38), 9775–9782. https://doi.org/10.1039/c5ob01451d

Otvos, J. D., Jeyarajah, E. J., Bennett, D. W., & Krauss, R. M. (1992). Development of a proton nuclear magnetic resonance spectroscopic method for determining plasma lipoprotein concentrations and subspecies distributions from a single, rapid measurement. *Clinical Chemistry*, *38*(9), 1632–1638. https://doi.org/10.1093/clinchem/38.9.1632

Otzen, D. E., Blans, K., Wang, H., Gilbert, G. E., & Rasmussen, J. T. (2012). Lactadherin binds to phosphatidylserine-containing vesicles in a two-step mechanism sensitive to vesicle size and composition. *Biochimica et Biophysica Acta*, *1818*(4), 1019–1027. https://doi.org/10.1016/j.bbamem.2011.08.032

Pedersbæk, D., Kræmer, M. K., Kempen, P. J., Ashley, J., Braesch-Andersen, S., Andresen, T. L., & Simonsen, J. B. (2019). The composition of reconstituted high-density lipoproteins (RHDL) dictates the degree of RHDL cargo- and size-remodeling via direct interactions with endogenous lipoproteins. *Bioconjugate Chemistry*, *30*(10), 2634–2646. https://doi.org/10.1021/acs.bioconjchem.9b00552

Phillips, Dr, Charo, If, Parise, Lv, & Fitzgerald, La (1988). The platelet membrane glycoprotein IIb-IIIa complex. *Blood*, *71*(4), 831–843

Pigault, C., Follenius-Wund, A., Schmutz, M., Freyssinet, J. -. M., & Brisson, A. (1994). Formation of two-dimensional arrays of annexin V on phosphatidylserine-containing liposomes. *Journal of Molecular Biology*, *236*(1), 199–208. https://doi.org/10.1006/jmbi.1994.1129

Rasmussen, R. W., Botha, J., Prip, F., Sanden, M., Nielsen, M. H., & Handberg, A. (2021). Zoom in on antibody aggregates: A potential pitfall in the search of rare EV populations. *Biomedicines*, *9*(2), 206. https://doi.org/10.3390/biomedicines9020206

Rupert, D. L. M., Mapar, M., Shelke, G. V., Norling, K., Elmeskog, M., Lötvall, J. O., Block, S., Bally, M., Agnarsson, B., & Höök, F. (2018).et al Effective refractive index and lipid content of extracellular vesicles revealed using optical waveguide scattering and fluorescence microscopy. *Langmuir: The ACS Journal of Surfaces and Colloids*, *34*(29), 8522–8531. https://doi.org/10.1021/acs.langmuir.7b04214

Shi, J., Heegaard, C. W., Rasmussen, J. T., & Gilbert, G. E. (2004). Lactadherin binds selectively to membranes containing phosphatidyl-L-serine and increased curvature. *Biochimica et Biophysica Acta*, *1667*(1), 82–90. https://doi.org/10.1016/j.bbamem.2004.09.006

Simonsen, J. B. (2017). What are we looking at? Extracellular vesicles, lipoproteins, or both? *Circulation Research*, *121*(8), 920–922. https://doi.org/10.1161/CIRCRESAHA.117.311767

Skotland, T., Sagini, K., Sandvig, K., & Llorente, A. (2020). An emerging focus on lipids in extracellular vesicles. *Advanced Drug Delivery Reviews*, *159*, 308–321. https://doi.org/10.1016/j.addr.2020.03.002

Sódar, B. W., Kittel, Á., Pálóczi, K., Vukman, K. V., Osteikoetxea, X., Szabó-Taylor, K., Németh, A., Sperlágh, B., Baranyai, T., Giricz, Z., Wiener, Z., Turiák, L., Drahos, L., Pállinger, É., Vékey, K., Ferdinandy, P., Falus, A., & Buzás, E. I. (2016). Low-density lipoprotein mimics blood plasma-derived exosomes and microvesicles during isolation and detection. *Scientific Reports*, *6*(April), 24316. https://doi.org/10.1038/srep24316

Steen, H. B. (1992). Noise, sensitivity, and resolution of flow cytometers. *Cytometry*, *13*(8), 822–830. https://doi.org/10.1002/cyto.990130804

Tian, Ye, Ma, L., Gong, M., Su, G., Zhu, S., Zhang, W., Wang, S., Li, Z., Chen, C., Li, L., Wu, L., & Yan, X. (2018). Protein profiling and sizing of extracellular vesicles from colorectal cancer patients via flow cytometry. *ACS Nano*, *12*(1), 671–680. https://doi.org/10.1021/acsnano.7b07782

Van Der Pol, E., Böing, A. N., Harrison, P., Sturk, A., & Nieuwland, R. (2012). Classification, functions, and clinical relevance of extracellular vesicles. *Pharmacological Reviews*, *64*(3), 676–705. https://doi.org/10.1124/pr.112.005983

Van Der Pol, E., De Rond, L., Coumans, F. A.W., Gool, E. L., Böing, A. N., Sturk, A., Nieuwland, R., & Van Leeuwen, T. G. (2018). Absolute sizing and label-free identification of extracellular vesicles by flow cytometry. *Nanomedicine: Nanotechnology, Biology, and Medicine*, *14*(3), 801–810. https://doi.org/10.1016/j.nano.2017.12.012

Van Der Pol, E., Hoekstra, A. G., Sturk, A., Otto, C., Van Leeuwen, T. G., & Nieuwland, R. (2010). Optical and non-optical methods for detection and characterization of microparticles and exosomes. *Journal of Thrombosis and Haemostasis: JTH*, *8*(12), 2596–2607. https://doi.org/10.1111/j.1538-7836.2010.04074.x

Varga, Z., Van Der Pol, E., Pálmai, M., Garcia-Diez, R., Gollwitzer, C., Krumrey, M., Fraikin, J. - L., Gasecka, A., Hajji, N., Van Leeuwen, T. G., & Nieuwland, R. (2018). Hollow organosilica beads as reference particles for optical detection of extracellular vesicles. *Journal of Thrombosis and Haemostasis: JTH*, *16*(8), 1646–1655. https://doi.org/10.1111/jth.14193

Welsh, J. A., Van Der Pol, E., Arkesteijn, G. J.A., Bremer, M., Brisson, A., Coumans, F., Dignat-George, F., Duggan, E., Ghiran, I., Giebel, B., Görgens, A., Hendrix, An, Lacroix, R., Lannigan, J., Libregts, S. F.W.M., Lozano-Andrés, E., Morales-Kastresana, A., Robert, S., De Rond, L., & …, Jones, J. C. (2020). MIFlowCyt-EV: A framework for standardized reporting of extracellular vesicle flow cytometry experiments. *Journal of Extracellular Vesicles*, *9*(1), 1713526. https://doi.org/10.1080/20013078.2020.1713526

Welton, J. L., Webber, J. P., Botos, L. -. A., Jones, M., & Clayton, A. (2015). Ready-made chromatography columns for extracellular vesicle isolation from plasma. *Journal of Extracellular Vesicles*, *4*, 27269. https://doi.org/10.3402/jev.v4.27269

Wojczynski, M. K., Glasser, S. P., Oberman, A., Kabagambe, E. K., Hopkins, P. N., Tsai, M. Y., Straka, R. J., Ordovas, J. M., & Arnett, D. K. (2011). High-fat meal effect on LDL, HDL, and VLDL particle size and number in the genetics of lipid-lowering drugs and diet network (GOLDN): An interventional study. *Lipids in Health and Disease*, *10*(3), 181. https://doi.org/10.1186/1476-511X-10-181

Yáñez-Mó, M., Siljander, P. R.-M., Andreu, Z., Bedina Zavec, A., Borràs, F. E., Buzas, E. I., Buzas, K., Casal, E., Cappello, F., Carvalho, J., Colás, E., Cordeiro-Da Silva, A., Fais, S., Falcon-Perez, J. M., Ghobrial, I. M., Giebel, B., Gimona, M., Graner, M., Gursel, I., & …, De Wever, O.(2015). Biological properties of extracellular vesicles and their physiological functions. *Journal of Extracellular Vesicles*, *4*, 1–60. https://doi.org/10.3402/jev.v4.27066

Yang, L. Y., Kuksis, A., Myher, J. J., Pang, H. (1992) Surface components of chylomicrons from rats fed glyceryl or alkyl esters of fatty acids: Minor components. *Lipids*, *27*(8), 613–618. https://doi.org/10.1007/BF02536119

SUPPORTING INFORMATION

Additional supporting information may be found in the online version of the article at the publisher's website.

How to cite this article: Botha, J., Handberg, A., & Simonsen, J. B. (2022). Lipid-based strategies used to identify extracellular vesicles in flow cytometry can be confounded by lipoproteins: Evaluations of annexin V, lactadherin, and detergent lysis. *Journal of Extracellular Vesicles*, *11,* e12200. https://doi.org/10.1002/jev2.12200